Supporting Information

Intercomparison of an Aerosol Chemical Speciation Monitor (ACSM) with Ambient Fine Aerosol Measurements in Downtown Atlanta, Georgia

S.H. Budisulistiorini[1], M.R. Canagaratna[2], P.L. Croteau[2], K. Baumann[3], E.S. Edgerton[3], M.S. Kollman[4], N.L. Ng[4,5], V. Verma[5], S.L. Shaw[6], E.M. Knipping[7], D.R. Worsnop[2], J.T. Jayne[2], R.J. Weber[5], and J.D. Surratt[1,*]

[1] Department of Environmental Sciences and Engineering, Gillings School of Global Public Health, The University of North Carolina at Chapel Hill, Chapel Hill, NC 27599, USA

[2] Aerodyne Research, Inc., Billerica, MA 01821, USA

[3] Atmospheric Research & Analysis, Inc., Cary, NC 27513, USA

[4] School of Chemical and Biomolecular Engineering, Georgia Institute of Technology, Atlanta, GA 30332, USA

[5] School of Earth and Atmospheric Sciences, Georgia Institute of Technology, Atlanta, GA 30332, USA

[6] Electric Power Research Institute, Palo Alto, CA 94304, USA

[7] Electric Power Research Institute, Washington, D.C. 20036, USA

[*]Correspondence to: J.D. Surratt (surratt@unc.edu)

A. ACSM Data Analysis

The ACSM has non-unit collection efficiency (CE) for sampled particles due to (i) transmission losses in the aerodynamic lenses, (ii) broadening of the particle beam; and (iii) particle bounce losses during impaction on the vaporizer (Huffman et al., 2005). These CE constraints are identical for both the ACSM and AMS instruments. Previous measurements have shown that an AMS CE of 0.5 reproduces ambient species mass concentrations to within 25% or better of measurements of collocated instruments (Canagaratna et al., 2007) and within 81-90% of fine aerosol volume or PILS measurements (Middlebrook et al., 2012). A

composition dependent CE parameterization account for higher CEs that are observed when the sampled ambient aerosol is acidic, has a high nitrate content, or is sampled under very humid conditions (Middlebrook et al., 2012). In this manuscript we use CE of 0.5 that was examined against composition dependent collection efficiency ($CE_{estimate}$) based on Middlebrook et al. (2012) parameterizations as follows:

a) Effect of high aerosol acidity:

$$\frac{NH_4^+{}_{measured}}{NH_4^+{}_{predicted}} = \frac{NH_4/18}{(SO_4/96)\times 2 + (NO_3/62) + (Chl/35.5)}$$

$$CE_{est,acidic} = 1.0 - 0.73 \times \left(NH_4^+{}_{meas}/NH_4^+{}_{predict}\right)$$

$$CE_{dry} = max\left(0.5, CE_{est,acidic}\right)$$

b) Effect of high ammonium nitrate fraction (ANMF):

$$ANMF = \frac{(80/62)\times NO_3}{(NH_4 + SO_4 + NO_3 + Chl + Org)}$$

$$CE_{est,ANMF} = 0.0833 + 0.9167 \times ANMF$$

$$CE_{dry} = max\left(0.5, CE_{est,ANMF}\right)$$

Observation of summer 2011 dataset suggests that only a few sporadic events were influenced by high aerosol acidity (Figure S1) which are attributed to low ammonium loadings. In addition, in fall 2011 where nitrate concentration was enhanced compared to summer measurements, suggests that CE was not affected by high ammonium nitrate fraction (Figure S2). Therefore, CE of 0.5 was used in analysis of all species for all dataset.

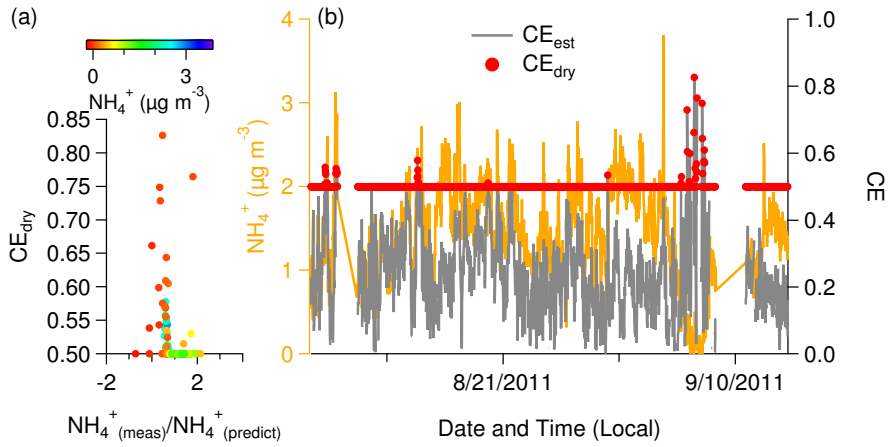

Figure S1. (a) CE_{dry} against $NH_4^+{}_{meas}/NH_4^+{}_{predict}$ color coded by concentration of ammonium, and (b) relationship between ammonium loading and CE_{dry} in the summer 2011.

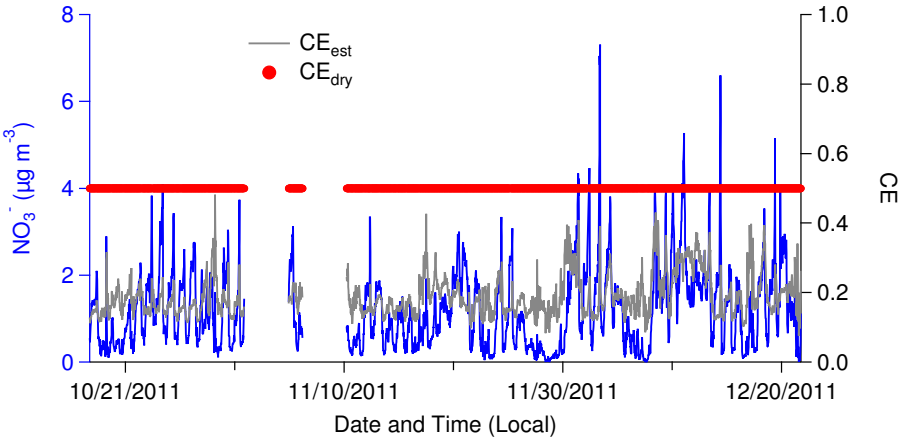

Figure S2. CE estimation based on nitrate loading during fall 2011.

Relative ionization efficiency (RIE) values were previously determined from laboratory calibrations with nitrate, ammonium, sulfate, and organics particles (Alfarra et al., 2004). Since the experiments for RIEs were conducted using AMS instrument, the values for ACSM might be different. It was found that for RIE of ammonium (RIE_{NH4}) that was 3.5, the value obtained from ACSM calibrations was between 5 and 6. RIE of sulfate might be estimated by fitting measured sulfate and predicted sulfate values. Measured sulfate ($SO_{4,meas}$) is sulfate that is measured by the ACSM, while predicted sulfate ($SO_{4,pred}$) is the estimated value of sulfate from ion balance approach. SO_{4pred} is derived from NH_{4pred} equation (N. L. Ng, personal communication, 2012) as follows:

$$NH_{4,pred} = 2\left(\frac{MW\ NH_4}{MW\ SO_4}\right) SO_{4,meas} + \left(\frac{MW\ NH_4}{MW\ NO_3}\right) NO_{3.meas} + \left(\frac{MW\ NH_4}{MW\ Chl}\right) Chl_{meas} \quad (1)$$

$$SO_{4,pred} = \frac{NH_{4,meas} - \left(\frac{MW\ NH4}{MW\ NO3}\right) NO_{3,meas} - \left(\frac{MW\ NH4}{MW\ Chl}\right) Chl_{meas}}{2\left(\frac{MW\ NH4}{MWSO4}\right)} \quad (2)$$

Previous value of RIE_{SO4} 1.5 is then multiplied by slope obtained from fitting $SO_{4,pred}$ versus $SO_{4,meas}$ and used as the RIE_{SO4} value of this study.

Maintenance issues included periods of complete instrument shutdown for calibration and start-up following calibration. During such start-up periods, vaporizer temperature, naphthalene signal, which serves as internal calibration, and airbeam signal showed instability, indicating that the ACSM was adjusting to operating conditions. An irregular naphthalene signal during continuous operation was also indicative of a problem, probably temporary clogging of the 1-µm pinhole of the naphthalene bath. Another operational issue encountered was a temporary disturbance in the electronic baseline (i.e., electronic zero value). Shifts in the electronic baseline might have occurred when there were short power outages at the JST site. Any of the described above were immediately reflected on the diagnostic panel, allowing precise determination of the sampling periods to be excluded from the data analysis.

B. JST Site Measurements

B.1 Integrated particle measurements

Integrated $PM_{2.5}$ sampling and analysis are listed in Table 2 and described briefly below. 24-h integrated $PM_{2.5}$ samples were collected using particle composition monitor (PCM) built by ARA that was specifically designed to minimize and/or account for potential artefacts and reactive gas interferences (Edgerton et al., 2005). PCM is a multichannel, sequential filter-based sampler that each consists of a teflon-coated cyclone (URG) with 10-mm cut size as the inlet, one or more denuder to remove gas interferences, Well Impactor Ninety-Six (WINS) with cut size of 2.5-mm, and filter media. Flow through each PCM's channel was maintained at 16.7 L min^{-1} using mass flow controllers (MFCs). There were three PCM channels that were sampling simultaneously. PCM1 channel was used for routine quantification of $PM_{2.5}$ mass, major ions, volatile nitrate (NO_3^-), volatile ammonium (NH_4^+), and trace elements. Series of denuders used in PCM1 channel were sodium bicarbonate ($NaHCO_3$) followed by citric acid ($C_6H_6O_7$) that remove HNO_3, SO_2, and NH_3. Filter media used in PCM1 are three stacks of filters comprising of a 47-mm diameter Teflon filter, 47-mm diameter Nylon filter, and lastly 47-mm diameter $C_6H_6O_7$-coated cellulose filter. PCM2 channel was used to quantify sulfate (SO_4^{2-}), total NO_3^-, and NH_4^+ but was discontinued in 2000 due to measurement redundancy to that of PCM1 channel. PCM3 channel was used for quantification of organic carbon (OC) and black carbon (BC). A 100-mm long by 30-mm ID carbon honeycomb denuder (MAST Carbon, Ltd., Guildford, U.K.) was used to remove semi-volatile gaseous organics in PCM3. Filter media used for PCM3 channel were two pre-baked 37-mm diameter quartz filters stacked together. OC on the back filter was considered as volatilization loss from OC on the front filter, therefore, the resulting value represent a lower limit for the actual OC concentrations.

Component mass loading from each filter was corrected by blank filter using SEARCH network-wide average loadings from field blanks, then the corrected loading was normalized by sampling volume (Edgerton et al., 2005). Blank correction had been shown to significantly influence the overall mass and OC loadings. Moreover, species that were at or below instrument detection limits, such as non-volatile NO_3^-, black carbon (BC), and major metal oxides, were found to have poor precisions for overall SEARCH measurements (Edgerton et al., 2005).

Mass is determined using best estimate (BE) method that attempts to calculate particle compositions based on their actual loading in the atmosphere. $PM_{2.5}$ mass is calculated from blank-corrected mass from FRM, PCM1 or TEOM and adding volatile NO_3^- from PCM1 Nylon,

volatile NH_4^+, and volatile OM from PCM back filter. NO_3^- is calculated as total NO_3^- from PCM1 Teflon filter + PCM1 Nylon filter. SO_4^{2-} calculation for BE method is identical to FRM method. NH_4^+ is calculated as total NH_4^+ that includes non-volatile NH_4^+ from PCM1 Teflon and volatile NH_4^+ that is estimated as 0.29 times the volatile NO_3^-. OC is calculated as the sum of front and back filters from PCM3. Since the back filter is assumed as volatilization product of the front filter and only 10% of them are analyzed, it is estimated as a quarterly ratio of OC from the back filter to OC from the front filter. These result in a formula for OC:

$$OC = OC_{front}\left(1 + R_q\right) \quad (1)$$

$$OM = OC \times 1.8 \quad (2)$$

where R_q is the estimated average ratio of volatile OC for quarter q. Particle compositions resulted from BE method estimation are used in this study as it represents the actual atmospheric loadings.

B.2 Continuous particle measurements

Details of continuous $PM_{2.5}$ sampling and analysis are provided in Edgerton et al. (2006) and listed in Table 2. Briefly, $PM_{2.5}$ mass is measured continuously using an R & P Model 1400 a/b TEOM operated at 30 °C to reduce losses of semivolatile compounds and main flow of 3 L min^{-1}. Sample air is pulled through PM_{10} inlet followed by $PM_{2.5}$ cyclone and goes inside the trailer where a multitube Nafion drier (Perma Pure) is installed to dry the sample.

SO_4^{2-} is measured continuously using a modified Harvard School of Public Health (HSPH). The method utilizes a stainless steel tube (300-mm section of 316 stainless steel) heated to >850 °C in a Lindberg/Blue M horizontal tube furnace to reduce particulate sulfate to gaseous sulfur dioxide (SO_2) that is detected by a Thermo-Environmental Instrument (TEI) Model 43s or 43ctl high-sensitivity, pulsed ultraviolet fluorescence SO_2 analyzer. Sample air is drawn through $PM_{2.5}$ cyclone (BGI) followed by two 30 mm of outer diameter (OD), 254 mm long sodium carbonate and citric acid coated annular denuders (URG) and a 30 mmOD, 100 mm long activated carbon honeycomb denuder (Novacarb, Mast Carbon, Ltd.) that remove SO_2, reduced sulfur gases, nitrogen oxides (NO_x) and volatile organic compounds (VOCs). Baseline of the analyzer is zeroed very 90 min by diverting sample air through an inline filter upstream the heated tube for 10 min to correct baseline drift.

NH_4^+ and NO_3^- were measured using a three-channel continuous differencing approached developed by ARA (Edgerton et al., 2006). Sample air is coming from the same

inlet and denuders system as SO_4^{2-} and the denuded sample is divided into three analytical channels. Channel 1 (CH1) provides instrument dark current and residual gas-phase NO_y that represents baseline signal that will be used for the downstream analyzer. Channel 2 (CH2) produces baseline NO_y signal and NO signal converted from particulate nitrogen species assuming nitrate is the only species in the signal. Channel 3 (CH3) oxidizes NH_4^+ to NO and NO_2, and reduces NO_3^-, NO_2, and residual NO_y to NO. TEI Model 42s or 42ctl NO-nitrogen oxide (NO_x) analyzer is installed downstream of the three-channel converters to measure NO from each converter by NO-ozone chemiluminescence method. Ammonium and nitrate are then determined as CH3-CH2 and CH2-CH1, respectively. A caveat of this approach is other particulate nitrogen compounds can be measured as ammonium and nitrate species as long as they are convertible to NO (Edgerton et al., 2006).

Total carbon (TC) is measured using the Sunset OC/EC analyzer. Sample air is drawn through a PM_{10} inlet at flow rate of 16.7 L min^{-1} followed by a $PM_{2.5}$ cyclone. Aerosol is first collected on one of two metal plate impactors with cut size of 0.14 mm aerodynamic diameter for 60-min period, and then sample is diverted to the second impactor while the first impactor is heated. Particulate carbon is converted to CO_2 through two temperature plateaus, i.e., 275 °C and 750 °C, and then detected by non-dispersive infrared absorption (NDIR). The instrument in calibrated using CO_2 in zero air and is zeroed with CO_2-free air (<5 ppm). TC is defined as the net carbon produced at the last temperature plateau (750 °C).

Black carbon (BC) or elemental carbon (EC) is measured using a Magee Scientific Model AE-16 single-beam aethalometer that measures EC based on attenuation of light at a wavelength of 880 nm. Sample air is pulled through a $PM_{2.5}$ cyclone at flow rate of 5-6 L min^{-1} followed by a Nafion drier and a quartz tape filter. The instrument is zeroed with an in-line ball valve and absolute filter for 15 min every day. The ambient concentration of EC is estimated based on the rate of attenuation change, sample flow rate, and the default bulk absorption coefficient from the manufacturer (16.6 m^2 g^{-1}).

Component mass concentrations from the continuous analyzers (hereafter referred as Level1 data) were then adjusted to match the filter-based data since the continuous analyzers had been shown to drift over time. The resulting filter-adjusted continuous data (hereafter referred as Level_2 data) had been shown to agree within 1:1 line with the filter-based measurements (Edgerton et al., 2006). With respect to carbon measurements, OC is calculated

as the difference between filter-adjusted TC and filter-adjusted EC, and OM is estimated according to Eq. 2.

C. Results of ACSM and collocated measurements at JST site

Table S1. Chemical characteristics of ambient aerosol mass and constituents at the JST site measured by JST site instruments presented as average concentration ± 1 standard deviation in μg m^{-3}.

Methods	Mass	OC	SO_4^{2-}	NO_3^-	NH_4^+	Cl^-	EC
JST Continuous[a]							
Summer 2011	13.67 ± 5.09	3.89 ± 1.14	3.78 ± 1.74	0.26 ± 0.18	1.34 ± 0.49	-	0.79 ± 0.50
Fall 2011	9.11 ± 5.58	3.34 ± 2.38	1.59 ± 1.27	0.67 ± 0.54	0.69 ± 0.34	-	0.99 ± 1.07
JST Filter[a]							
Summer 2011	13.23 ± 5.21	3.78 ± 1.17	3.65 ± 1.34	0.25 ± 0.05	1.25 ± 0.47	0.03 ± 0.01	0.74 ± 0.29
Fall 2011	9.85 ± 4.40	3.86 ± 1.55	1.57 ± 0.74	0.48 ± 0.36	0.68 ± 0.30	0.05 ± 0.05	0.98 ± 0.78

[a] JST measures $PM_{2.5}$ mass and chemical constituents.

Table S2. Ambient aerosol mass concentrations measured by the integrated FRM methods presented in average concentration ± 1 standard deviation.

	FRM Filters	
	PM_1 (μg m^{-3})	$PM_{2.5}$ (μg m^{-3})
Winter 2011	8.08 ± 3.44	9.10 ± 3.85
Spring 2012	8.58 ± 2.67	9.71 ± 3.01
Summer 2012	8.71 ± 2.65	10.38 ± 3.02

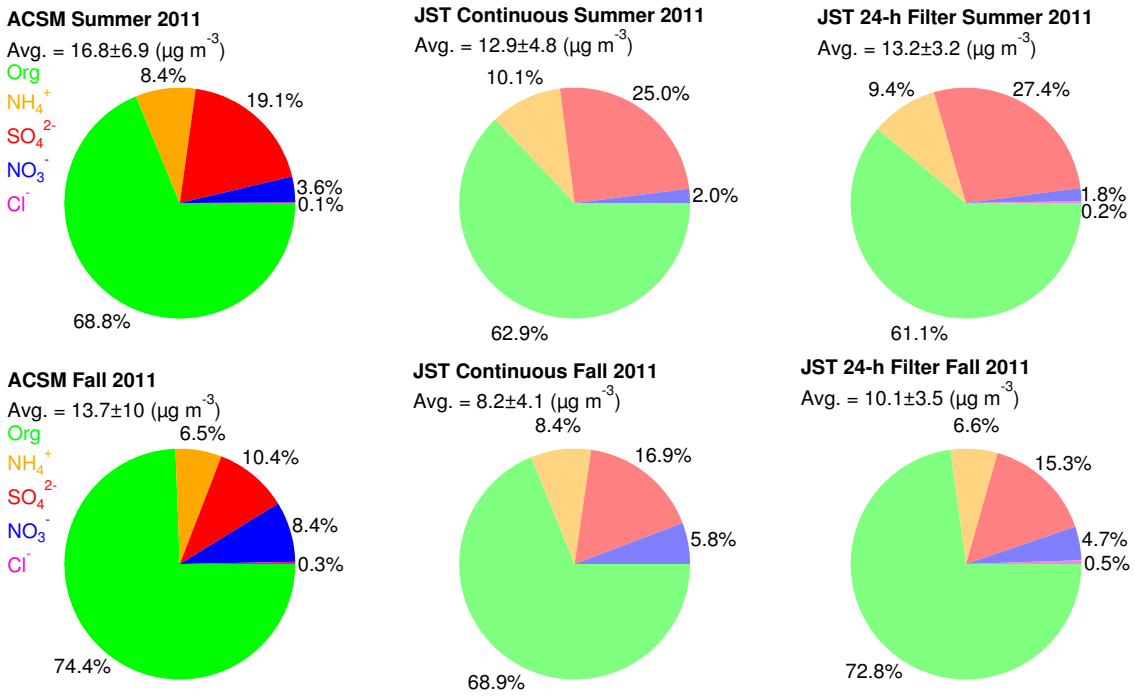

Figure S3. Pie charts of speciated aerosol measurements from the ACSM and JST. Pie charts in sharp colors are the ACSM, while the blur colors indicate other measurement techniques. Organic fraction of filter-adjusted continuous data was calculated from OC measurement multiplied by 1.8, which is ratio of OM/OC. For the 24-h filter-based data, it was calculated from OC measurement multiplied by 1.8 and correction values (SAF), that are 1.13 and 1.07 for periods of July–September and October–December, respectively. ACSM measures PM_1 while JST measures $PM_{2.5}$. Average $PM_{2.5}$ mass for 24-h filter based measurement was calculated from five species (i.e., OM, NH_4^+, SO_4^{2-}, NO_3^-, and Cl^-), hence it excluded contribution from other anions such as Na^+, Mg^+, K^+, and Ca^+. Calculation of average $PM_{2.5}$ mass for continuous measurement did not include chloride and other anions as they are not available.

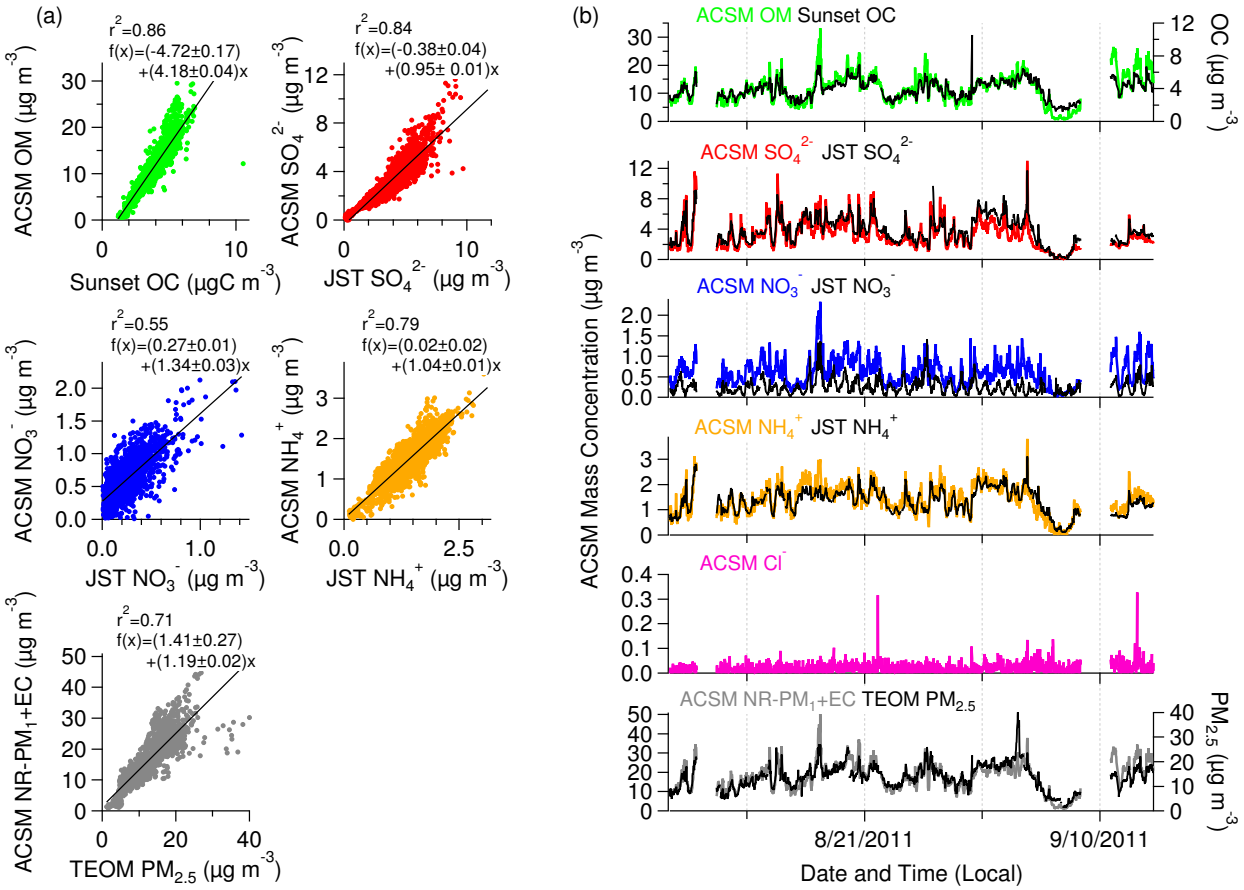

Figure S4. (a) Linear regression correlation and (b) time series plots of organic and inorganic constituents measured by the UNC ACSM and collocated measurements at JST site during summer 2011.

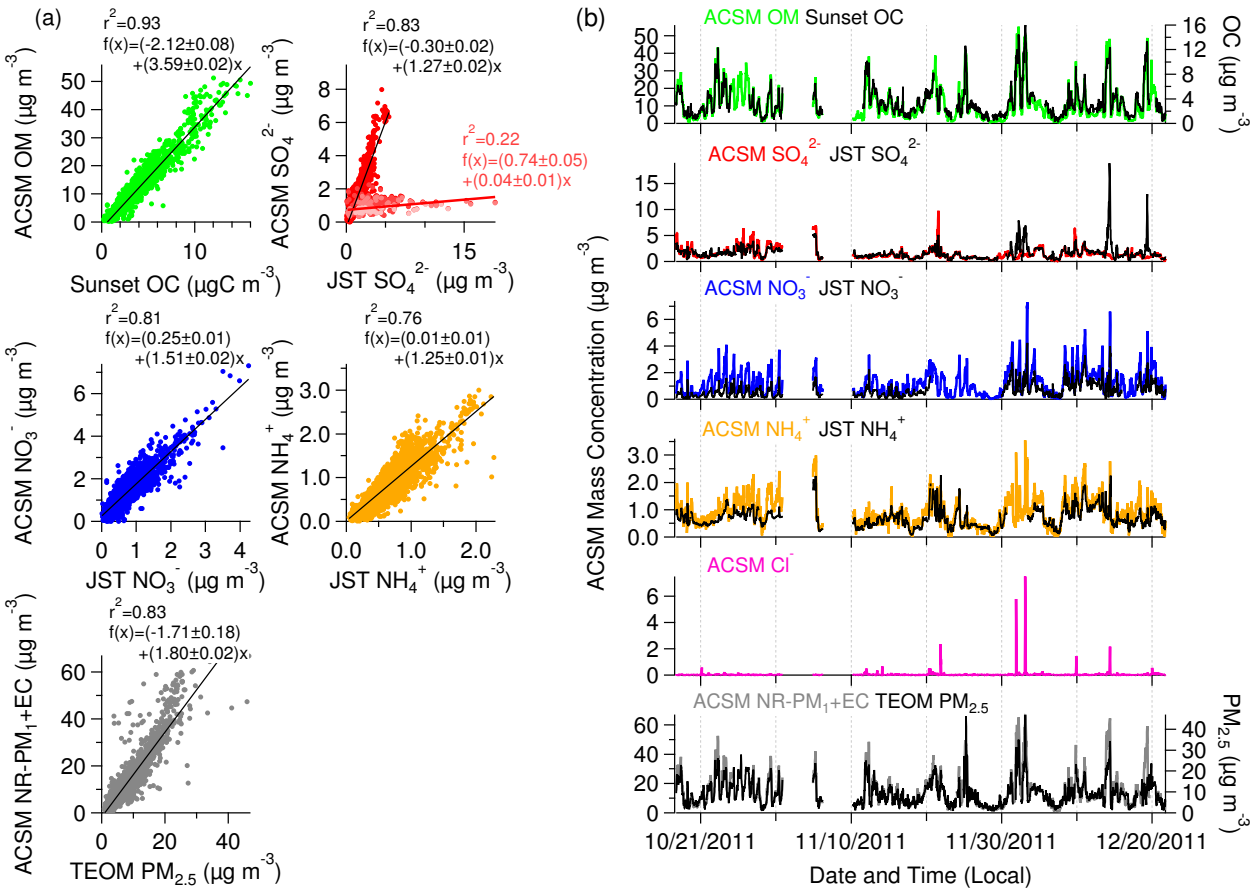

Figure S5. (a) Linear regression correlation and (b) time series plots of organic and inorganic constituents measured by the UNC ACSM and collocated measurements at JST site during fall 2011.

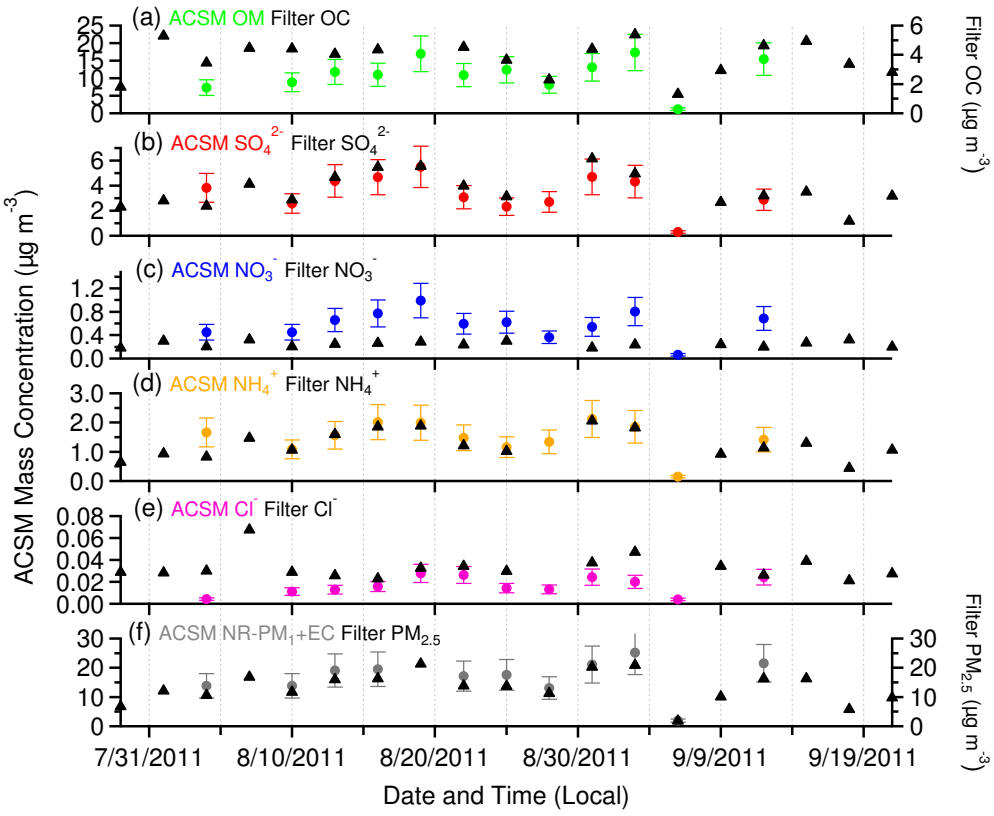

Figure S6. Time series plots with 30% of uncertainty of organic (OM vs. OC), inorganics constituents (SO_4^{2-}, NO_3^-, NH_4^+, and Cl^-), and mass concentrations measured by the UNC ACSM and the JST 24-h filter measurement during summer period.

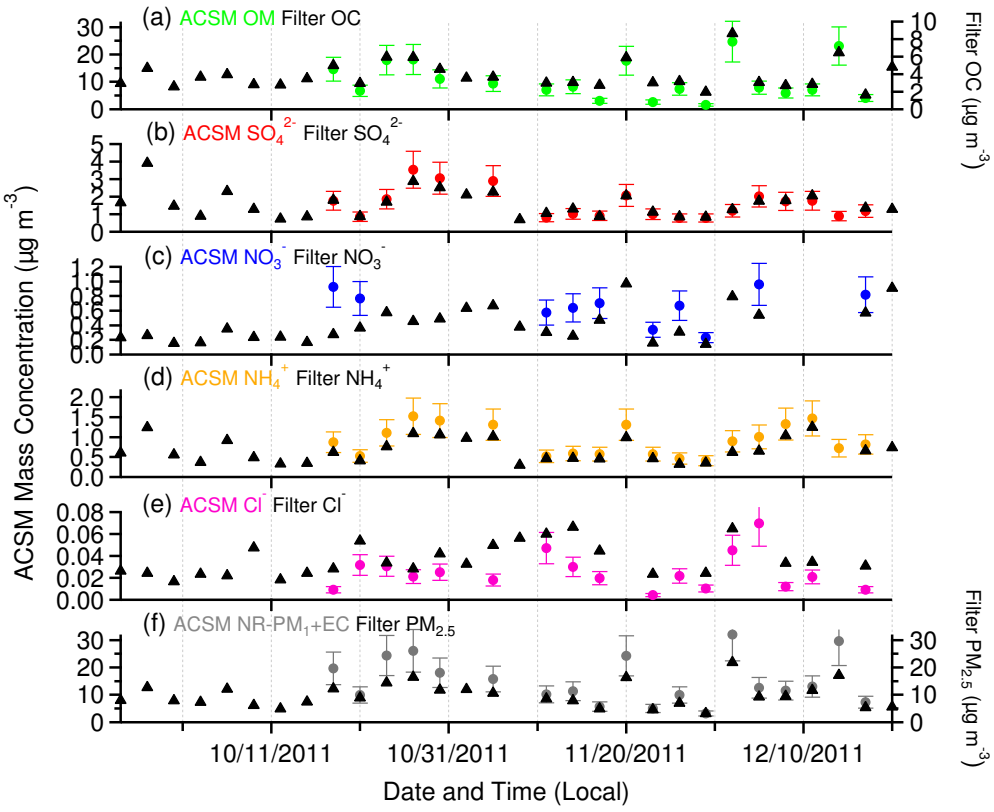

Figure S7. Time series plots with 30% of uncertainty of organic (OM vs. OC), inorganics constituents (SO_4^{2-}, NO_3^-, NH_4^+, and Cl^-), and mass concentrations measured by the UNC ACSM and the JST 24-h filter measurement during fall period.

D. Influence of organic nitrate component to ACSM NO_3^- signal

Discrepancies in the ACSM NO_3^- and the continuous measurements might also be attributable to the overall low concentrations of NO_3^- in summer where both measurements are near their detection limits. ACSM NO_3^- measurements are based on the measured *m/z* 30 and *m/z* 46 ion signals. At low concentrations, small contributions to the *m/z* 30 signal can also originate from organic nitrates (NO^+), oxygenated organics (CH_2O^+), and/or organic-nitrate compounds (CH_4N^+) that are not precisely accounted for. This *m/z* 30 interference can result in higher reported values for inorganic nitrate (as measured from NO^+ (*m/z* 30) and NO_2^+ (*m/z* 46)) (Marcolli et al., 2006, Bae et al., 2007). Contribution of sum of organic and inorganic nitrate can be significant to total secondary organic aerosol (SOA), although, Rastogi et al. (2011) suggested that contribution of water soluble nitrogenous organic compounds is not significant during summer in the southeastern U.S.

To investigate aerosol acidity influence to NO_3^- measurement, time series traces of ACSM NO_3^- colour coded by degree of neutralization calculated according to Zhang et al. (2007), and JST NO_3^- measured in summer and fall are presented in Figures S9 and S10, respectively. Most of the time, the aerosol is slightly acidic (ratio of NH_4^+ to $SO_4^{2-} + NO_3^- + Cl^-$ < 1) in summer, suggesting that nitrate concentration in ambient acidic aerosol is usually low due to HNO_3 displacement by H_2SO_4 (Zhang et al., 2005b). In contrast, during fall season the aerosol is less acidic (ratio > 1) and the nitrate concentration is higher. The linear correlations of *m/z* 30 and 46 from the ACSM NO_3^- with JST NO_3^- are moderate in summer ($r^2 = 0.5$), but they are stronger in fall ($r^2 \geq 0.6$). Interestingly, while linear regression slope of *m/z* 30 versus JST NO_3^- was decreasing from summer to fall (1.58 to 1.31), slopes of m/z 46 were relatively constant between these two seasons (0.36 to 0.34). These may suggest that the *m/z* 30 ion measured by the ACSM is likely being influenced by fragments other than NO_3^- compared to that of *m/z* 46. In order to investigate the influence of organic or oxygenated organic species to *m/z* 30, time series traces of excess of *m/z* 30 signal (Δ*m/z* 30) calculated by formula provided in Bae et al. (2007) in the summer and fall are presented in Figures S10 and S11, respectively. The Δ*m/z* 30, which is suggested to be derived from organic-related or organic nitrate-related *m/z* 30 (Bae et al., 2007), has positive values most of time, but the signal is lower in summer (Figure S10a) than in fall (Figure S11a). During both seasons, the linear correlations between Δ*m/z* 30 and the HOA factor (Figures S10b and S11b) derived from positive matrix factorization (PMF) analysis of the ACSM organic fraction (Budisulistiorini et al., 2013) are weak ($r^2 < 0.2$), but they are better for correlations with OOA factor (Figures S10c and S11c). HOA factor is

mainly attributed to organic aerosol formed from primary emissions and mass spectra are dominated by ions identical with hydrocarbons. On the other hand, OOA factor is characterized by mass spectra dominated by oxygenated ion fragments, and thus linked to SOA (Zhang et al., 2005a). The moderate correlation of $\Delta m/z$ 30 with OOA factor (r^2 = 0.5) in the fall might indicate that the *m/z* 30 signals measured by the ACSM are influenced by oxygenated organic species.

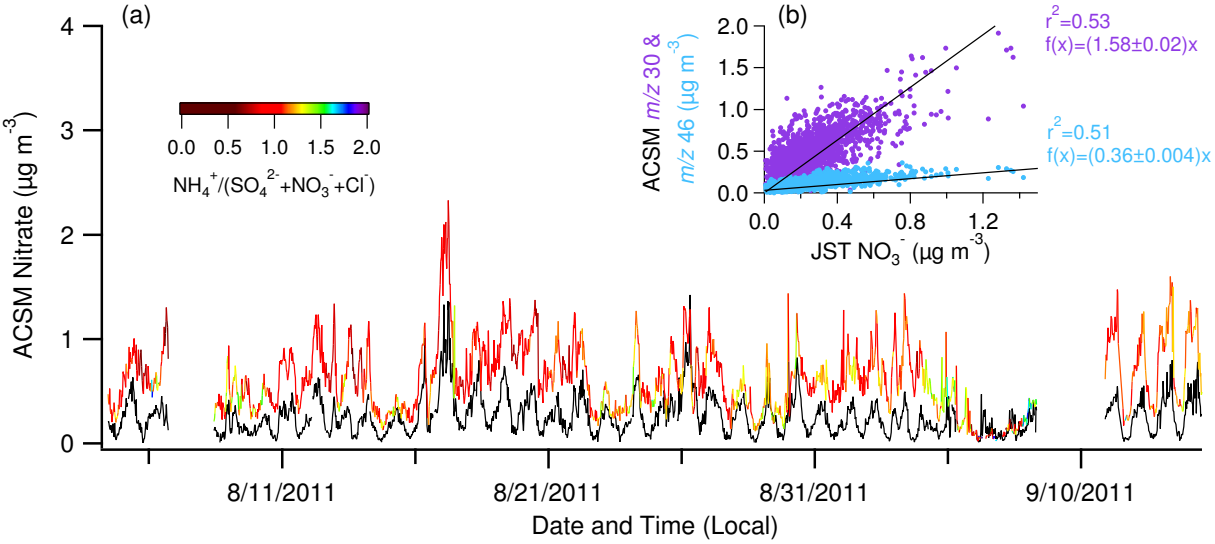

Figure S8. (a) Time series traces of the ACSM nitrate color coded by degree of neutralization and JST nitrate (black line), and (b) correlation scatterplot between the ACSM nitrate ion tracers, i.e., *m/z* 30 and 46, and JST nitrate for summer 2011 period.

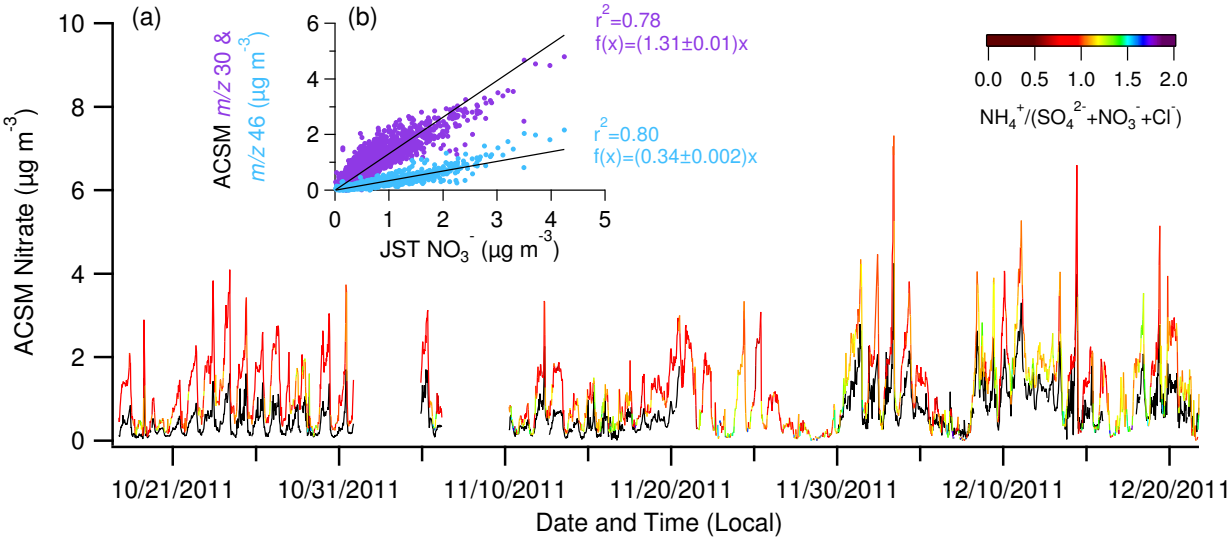

Figure S9. (a) Time series traces of the ACSM nitrate color coded by degree of neutralization and JST nitrate (black line), and (b) correlation scatterplot between the ACSM nitrate ion tracers, i.e., *m/z* 30 and 46, and JST nitrate for fall 2011 period.

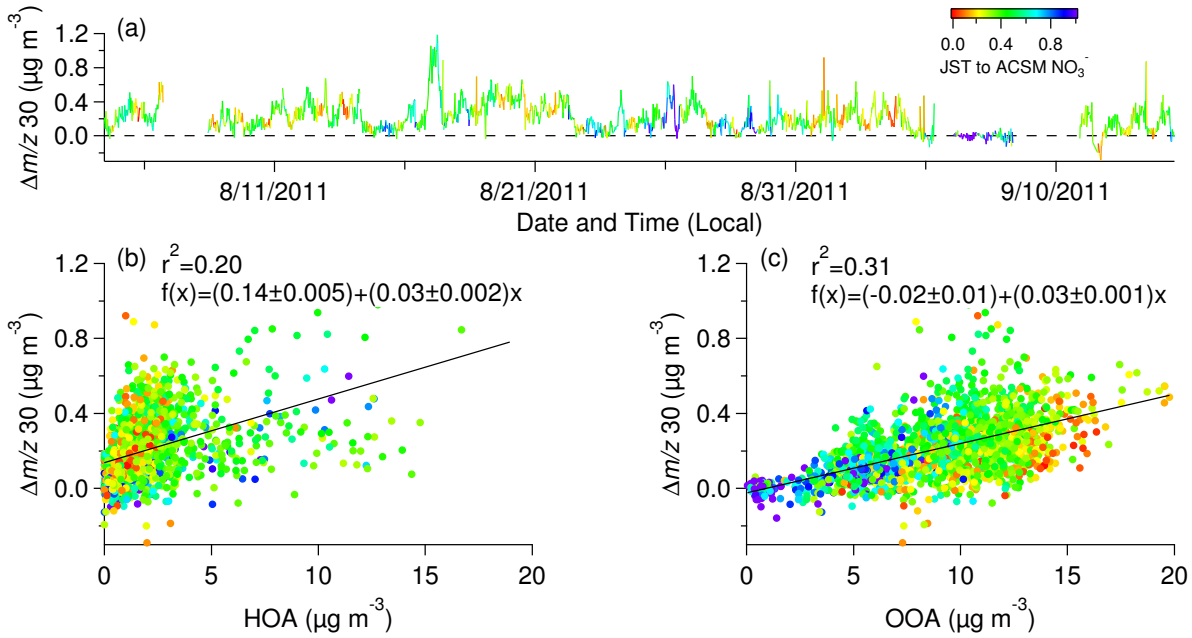

Figure S10. (a) Time series traces of the ACSM nitrate color coded by ratio of JST nitrate to ACSM nitrate, and correlation scatterplot between estimated *m/z* 30 signal excess attributed to organic-linked (Δ*m/z* 30 mass) and (b) HOA and (c) OOA (= LV-OOA + SV-OOA + IEPOX-OA) factors from PMF analysis for summer 2011 period.

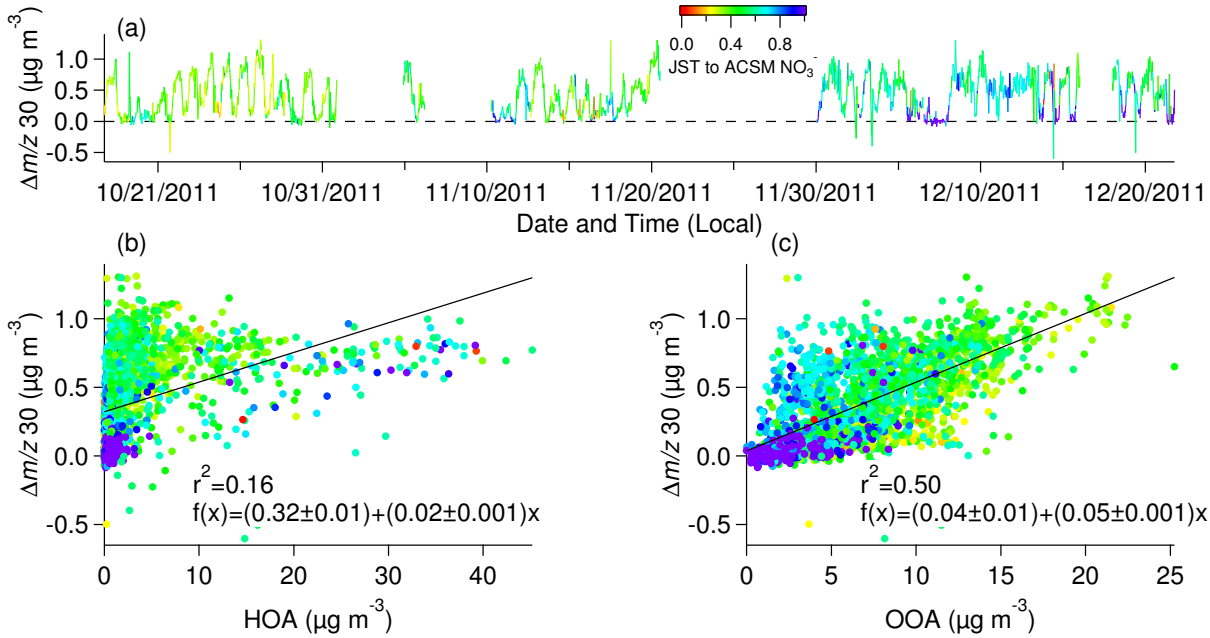

Figure S11. (a) Time series traces of the ACSM nitrate color coded by ratio of JST nitrate to ACSM nitrate, and correlation scatterplot between estimated *m/z* 30 signal excess attributed to

organic-linked (Δ*m/z* 30 mass) and (b) HOA and (c) OOA (= LV-OOA + SV-OOA) factors from PMF analysis for fall 2011 period.

References

Alfarra, M. R., Coe, H., Allan, J.D., Bower, K.N., Boudries, H., Canagaratna, M.R., Jimenez, J.L., Jayne, J.T., Garforth, A.A., Li, S. and Worsnop, D.R.: Characterization of urban and rural organic particulate in the Lower Fraser Valley using two Aerodyne Aerosol Mass Spectrometers, Atmos.Environ., 38, 5745-5758, doi:10.1016/j.atmosenv.2004.01.054, 2004.

Bae, M., Schwab, J.J., Zhang, Q., Hogrefe, O., Demerjian, K.L., Weimer, S., Rhoads, K., Orsini, D., Venkatachari, P. and Hopke, P.K.: Interference of organic signals in highly time resolved nitrate measurements by low mass resolution aerosol mass spectrometry, 112, - D22305, doi:10.1029/2007JD008614, 2007.

Budisulistiorini, S. H., Canagaratna, M.R., Croteau, P.L., Marth, W.J., Baumann, K., Edgerton, E.S., Shaw, S.L., Knipping, E.M., Worsnop, D.R., Jayne, J.T., Gold, A. and Surratt, J.D.: Real-Time Continuous Characterization of Secondary Organic Aerosol Derived from Isoprene Epoxydiols in Downtown Atlanta, Georgia, Using the Aerodyne Aerosol Chemical Speciation Monitor, Environ.Sci.Technol., 47, 5686-5694, doi:10.1021/es400023n, 2013.

Canagaratna, M. R., Jayne, J.T., Jimenez, J.L., Allan, J.D., Alfarra, M.R., Zhang, Q., Onasch, T.B., Drewnick, F., Coe, H., Middlebrook, A., Delia, A., Williams, L.R., Trimborn, A.M., Northway, M.J., DeCarlo, P.F., Kolb, C.E., Davidovits, P. and Worsnop, D.R.: Chemical and microphysical characterization of ambient aerosols with the aerodyne aerosol mass spectrometer, Mass Spectrom.Rev., 26, 185-222, doi:10.1002/mas.20115, 2007.

Edgerton, E. S., Hartsell, B.E., Saylor, R.D., Jansen, J.J., Hansen, D.A. and Hidy, G.M.: The Southeastern Aerosol Research and Characterization Study, Part 3: Continuous Measurements of Fine Particulate Matter Mass and Composition, J.Air Waste Manage.Assoc., 56, 1325-1341, 2006.

Edgerton, E. S., Hartsell, B.E., Saylor, R.D., Jansen, J.J., Hansen, D.A. and Hidy, G.M.: The Southeastern Aerosol Research and Characterization Study: Part II. Filter-Based Measurements of Fine and Coarse Particulate Matter Mass and Composition, J.Air Waste Manage.Assoc., 55, 1527-1542, 2005.

Huffman, J. A., Jayne, J.T., Drewnick, F., Aiken, A.C., Onasch, T., Worsnop, D.R. and Jimenez, J.L.: Design, Modeling, Optimization, and Experimental Tests of a Particle Beam Width Probe for the Aerodyne Aerosol Mass Spectrometer, 39, 1143-1163, doi:10.1080/02786820500423782, 2005.

Marcolli, C., Canagaratna, M.R., Worsnop, D.R., Bahreini, R., de Gouw, J.A., Warneke, C., Goldan, P.D., Kuster, W.C., Williams, E.J., Lerner, B.M., Roberts, J.M., Meagher, J.F., Fehsenfeld, F.C., Marchewka, M., Bertman, S.B. and Middlebrook, A.M.: Cluster Analysis of the Organic Peaks in Bulk Mass Spectra Obtained During the 2002 New England Air Quality Study with an Aerodyne Aerosol Mass Spectrometer, 6, 5649-5666, doi:10.5194/acp-6-5649-2006, 2006.

Middlebrook, A. M., Bahreini, R., Jimenez, J.L. and Canagaratna, M.R.: Evaluation of Composition-Dependent Collection Efficiencies for the Aerodyne Aerosol Mass Spectrometer using Field Data, 46, 258-271, doi:10.1080/02786826.2011.620041, 2012.

Rastogi, N., Zhang, X., Edgerton, E.S., Ingall, E. and Weber, R.J.: Filterable water-soluble organic nitrogen in fine particles over the southeastern USA during summer, Atmos.Environ., 45, 6040-6047, doi:10.1016/j.atmosenv.2011.07.045, 2011.

Zhang, Q., Alfarra, M.R., Worsnop, D.R., Allan, J.D., Coe, H., Canagaratna, M.R. and Jimenez, J.L.: Deconvolution and Quantification of Hydrocarbon-like and Oxygenated Organic Aerosols Based on Aerosol Mass Spectrometry, Environ. Sci. Technol., 39, 4938-4952, doi:10.1021/es048568l, 2005a.

Zhang, Q., Canagaratna, M.R., Jayne, J.T., Worsnop, D.R. and Jimenez, J.: Time- and size-resolved chemical composition of submicron particles in Pittsburgh: Implications for aerosol sources and processes, J.Geophys.Res., 110, D07S09, doi:10.1029/2004JD004649, 2005b.

Zhang, Q., Jimenez, J.L., Worsnop, D.R. and Canagaratna, M.: A Case Study of Urban Particle Acidity and Its Influence on Secondary Organic Aerosol, Environ. Sci. Technol., 41, 3213-3219, doi:10.1021/es061812j, 2007.